Contribution from the Department of Inorganic Chemistry,
University of Sydney, Sydney 2006, Australia

Structure and Properties of a Dimeric Hydroxo-Bridged Ytterbium(III) Complex, Di-μ-hydroxo-bis[triaquo(pyridine-2-carboxaldehyde 2′-pyridylhydrazone)ytterbium(III)] Tetrachloride Tetrahydrate

EVELINE BARANIAK, ROBERT ST. L. BRUCE, HANS C. FREEMAN,* NEIL J. HAIR, and JULIA JAMES

Received February 12, 1976 AIC601129

An x-ray crystal structure analysis shows that a complex between ytterbium(III) and pyridine-2-carboxaldehyde 2′-pyridylhydrazone (paphy) is a centrosymmetric dimer. The complex, $[Yb(paphy)(H_2O)_3(OH)]_2Cl_4{\cdot}4H_2O$ = $[YbC_{11}H_{17}N_4O_4]_2Cl_4{\cdot}4H_2O$, crystallizes with an orthorhombic unit cell, a = 15.70 (2), b = 11.81 (1), c = 20.35 (2) Å, Z = 4, space group *Pbca*. The measured and calculated densities are d_m = 1.92 (1) and d_x = 1.93 g cm^{-3}, respectively. The structure has been refined by full-matrix least squares to a residual 0.052 for 1678 reflections recorded with Cu Kα radiation on an equiinclination diffractometer. The ytterbium(III) atoms are eight coordinate, with the donor atoms arranged around them in an approximate dodecahedron. The two ytterbium atoms of each dimer form a planar four-membered ring with two bridging hydroxyl ions. The paphy molecules act as tridentate ligands. They are nonplanar, the dihedral angle between the two pyridine rings in each ligand being 15°. The metal–ligand bond lengths are: Yb–N(pyridine) = 2.49 (1), 2.52 (1) Å; Yb–N(imine) = 2.54 (1) Å; Yb–O(hydroxyl) = 2.19 (1), 2.22 (1) Å; Yb–O(water) = 2.33 (1), 2.34 (1), 2.42 (1) Å. The results of the structure analysis are consistent with the infrared and uv–visible spectra and with the magnetic susceptibility of the complex.

Introduction

A number of lanthanide complexes have been prepared from the neutral nitrogen donor ligand, pyridine-2-carboxaldehyde 2′-pyridylhydrazone ($C_5H_4N{-}CH{=}N{-}NH{-}C_5H_4N$ = paphy), using ethanol as the solvent.[1] We here report the structural, magnetic, and spectroscopic study of one of these complexes, namely $[Yb(paphy)(H_2O)_3(OH)]_2Cl_4{\cdot}4H_2O$.

Experimental Section

Preparation of $[Yb(paphy)(H_2O)_3(OH)]_2Cl_4{\cdot}4H_2O$. Ytterbium(III) oxide (Fluka, 99.9%) was dissolved in concentrated hydrochloric acid. Excess acid was removed by evaporation on a steam bath, giving a crystalline product of hydrated ytterbium(III) chloride. Filtered, saturated solutions of the hydrated metal chloride (1.4 g, 4×10^{-3} mol) and paphy (0.8 g, 4.4×10^{-3} mol) in ethanol were mixed. The final volume was approximately 10 ml. The mixture was boiled on a steam bath for 5 min and was then allowed to stand at room temperature. After 24 h the pale-yellow, crystalline product was collected, washed with cold ethanol, dried by suction, and allowed to stand in a desiccator over silica gel for 48 h. Anal. Calcd for $YbC_{11}H_{21}N_4O_6Cl_2$: C, 24.0; H, 3.9; N, 10.2; Cl, 12.9. Found: C, 24.0; H, 3.8; N, 10.3; Cl, 12.7.

Preparation of Mono- and Anhydrate. On being heated for 8 h in a vacuum oven at 70 °C (10 mm), the preceding compound showed a weight loss equivalent to two H_2O per Yb atom. Continued heating for 12 h at 180 °C and atmospheric pressure led to the loss of two more H_2O per Yb atom. Anal. Calcd for $YbC_{11}H_{13}N_4O_2Cl_2$: C, 27.7; H, 2.8; N, 11.8. Found: C, 28.0; H, 3.0; N, 12.0. These results are consistent with original, intermediate, and final compounds having stoichiometries $Yb(paphy)(H_2O)_3(OH)Cl_2{\cdot}2H_2O$, $Yb(paphy)(H_2O)_3(OH)Cl_2$, and $Yb(paphy)(H_2O)(OH)Cl_2$, respectively.

Physical Measurements. Infrared spectra in the region 4000–250 cm^{-1} were recorded on a Perkin-Elmer 459 spectrophotometer, using Nujol or hexachlorobutadiene mulls or CsBr disks. A Hitachi FIS-3 spectrophotometer was used for measurements in the region 400–30 cm^{-1}, the samples being thick Nujol mulls on a single polythene plate. A Unicam SP700 instrument was used to record diffuse transmittance spectra in the ultraviolet and visible range from Nujol mulls supported on Whatman No. 1 filter paper. Magnetic susceptibility measurements were made by the Gouy method between 90 and 340 K, using tris(ethylenediamine)nickel(II) thiosulfate as the calibrant. Diamagnetic corrections were made using Pascal's constants.[2] Elemental analyses were performed by the Australian Microanalytical Service, CSIRO, Melbourne.

Crystal Data. $[C_{11}H_{21}N_4O_6Cl_2Yb]_2$, fw = 1098.6, orthorhombic, a = 15.70 (2), b = 11.81 (1), c = 20.35 (2) Å, U = 3773 (7) Å^3, d_m = 1.92 (1) g cm^{-3} (by flotation in bromoform–ethanol), d_x = 1.93 g cm^{-3}, Z = 4. Space group *Pbca* (No. 61), from systematic absences of reflections ($0kl$ absent for $k = 2n + 1$, $h0l$ absent for $l = 2n + 1$, $hk0$ absent for $h = 2n + 1$).

The unit-cell dimensions were calculated directly from the values of the Bragg angles of a number of axial reflexions. The angles were measured on an equiinclination diffractometer with Ni-filtered Cu Kα radiation [λ(Cu Kα_1) = 1.5405, λ(Cu Kα_2) = 1.5443 Å]. Two crystals, mounted for rotation about the a and b axis, respectively, were used for the determination. The quoted esd's are the minimum changes in unit-cell dimensions which produced measurable missettings of high-angle reflections.

X-Ray Data. The intensities of 3265 independent x-ray reflections, including 1587 which were below the observable threshold, were recorded on a computer-controlled Buerger-Supper equiinclination diffractometer.[3] Ni-filtered Cu Kα x radiation from a fully stabilized generator, a scintillation counter (Philips PW1964/10), and pulse-height analyzer (PW 4280) were used. The reflections Hkl ($0 \le H \le 12$) and hKl ($0 \le K \le 10$) accessible in the range $15° < T < 140°$ were recorded from two crystal specimens. The maximum dimensions of the crystals were 0.13 × 0.17 × 0.09 mm and 0.10 × 0.12 × 0.04 mm, respectively, parallel to the a, b, and c axes. The counter apertures were selected to increase approximately linearly with the equiinclination angle μ. The angles which they subtended at the specimens for both the a- and b-axis data ranged from 2° 50′ (for the zero layer) to 4° 20′ (for the highest layer).

The intensities were recorded by the ω-scan method, using optimized scan ranges and including a test for background imbalance.[3] The scan-speed parameters as defined in ref 3 were ϕ'_{fast} = 0.333 deg s^{-1}, ϕ'_{min} = 0.05 deg s^{-1} for the a-axis data, and ϕ'_{fast} = ϕ'_{min} = 0.04 deg s^{-1} for the b-axis data. These parameters led to minimum and maximum scan times of 4.9 and 110 s per reflection, respectively. For each reflection, the intensity I and its variance $\sigma^2(I)$ were calculated from the expressions $I = N - B$ and $\sigma^2(I) = N + B$, where N is the integrated peak count and B is the sum of background counts (each made for half the time taken to scan the peak) at the two extremes of the scan. In the a-axis data set, any reflection whose intensity had a percentage variance in excess of an expectation value R_e = 0.03 was remeasured at a slower calculated scan speed. A reflection was considered to be unobserved if $I \le 1.6\sigma(I)$. In this event the intensity was replaced by $I_{unobsd} = 0.33I_{min}$ and its variance by $\sigma^2(I_{unobsd}) = 0.29I_{min}$,[4] where $I_{min} = 1.6\sigma(I)$.

Corrections for the Lorentz–polarization factors and for absorption were applied. The absorption corrections were calculated by the method of Coppens, Leiserowitz, and Rabinovich[5] for an 8 × 8 × 4 grid (parallel to a, b, and c) in the case of the crystal used to record the Hkl data, and for a 6 × 6 × 4 grid in the case of the crystal used to record the hKl data. The ranges of the transmission coefficients of the two crystals were 0.31–0.40 and 0.31–0.41, respectively (μ(Cu Kα) = 134 cm^{-1}). The absorption-corrected intensities were then brought to a common scale by using the least-squares method of Rae[6]

Table I. Atomic Positional Coordinates[a] and Anisotropic Thermal Parameters[a,b] in $[Yb(paphy)(H_2O)_3(OH)]_2Cl_4 \cdot 4H_2O$

Atom	10^4x	10^4y	10^4z	10^4U_{11}	10^4U_{22}	10^4U_{33}	10^4U_{12}	10^4U_{13}	10^4U_{23}
Yb	638.7(3)	14(1)	737.2(3)	223(3)	263(3)	199(3)	1(3)	-2(2)	32(3)
Cl(1)	2455(3)	366(3)	3930(2)	433(20)	471(24)	362(17)	-4(9)	-26(9)	25(8)
Cl(2)	1876(3)	3478(4)	1649(2)	467(24)	587(27)	440(22)	-118(12)	-58(10)	45(11)

Atom	10^4x	10^4y	10^4z	10^3U_{iso}	Atom	10^4x	10^4y	10^4z	10^3U_{iso}
O(1)	-670(5)	125(9)	335(3)	23(2)	C(1)	1047(11)	-2650(14)	200(8)	41(4)
O(2)	1487(6)	-4(12)	1685(4)	38(2)	C(2)	1036(11)	-3843(14)	154(8)	42(4)
O(3)	2088(7)	-466(9)	437(5)	41(3)	C(3)	590(14)	-4441(18)	596(10)	64(5)
O(4)	1213(7)	1795(9)	534(5)	42(3)	C(4)	200(13)	-3878(17)	1116(10)	58(5)
O(5)	1557(8)	1483(10)	2684(6)	54(3)	C(5)	203(9)	-2697(11)	1136(6)	22(3)
O(6)	1953(9)	2858(11)	4377(6)	66(4)	C(6)	-570(10)	-460(12)	2069(7)	26(3)
N(1)	640(8)	-2093(9)	679(6)	30(3)	C(7)	-668(12)	805(13)	1994(8)	33(4)
N(2)	-214(10)	-972(11)	1631(7)	36(4)	C(8)	-1208(10)	1413(13)	2416(7)	33(4)
N(3)	-164(8)	1280(10)	1516(5)	22(3)	C(9)	-1328(12)	2541(16)	2323(9)	54(5)
N(4)	-195(8)	-2116(11)	1622(6)	31(3)	C(10)	-842(11)	3063(15)	1819(8)	46(5)
					C(11)	-306(12)	2428(16)	1425(9)	44(5)

[a] In this and all subsequent tables, a number in parentheses represents the standard deviation right adjusted to the least significant digit of the preceding quantity. [b] The form of the anisotropic temperature factor is $\exp\{-2\pi^2(h^2a^{*2}U_{11} + k^2b^{*2}U_{22} + l^2c^{*2}U_{33} + 2hka^*b^*U_{12} + 2hla^*c^*U_{13} + 2klb^*c^*U_{23})\}$.

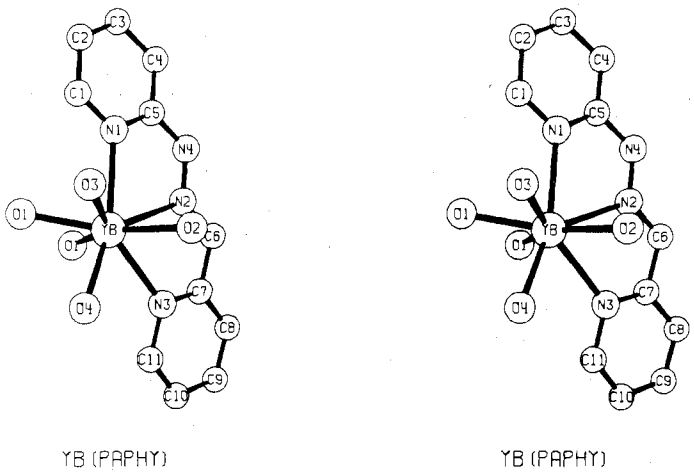

Figure 1. Stereoscopic drawing of one Yb atom and its coordination in $[Yb(paphy)(H_2O)_3(OH)]_2Cl_4 \cdot 4H_2O$.

to fit scale factors for the intersecting reciprocal lattice layers to the intensities of those reflections which were common to both data sets. The uncertainties (~1%) in the layer scale factors were taken into account in calculating the estimated standard deviations $\sigma(F_o)$ of the structure amplitudes $|F_o|$.

Crystal Structure Analysis and Refinement. The structure was solved by standard Patterson and Fourier methods. The function minimized in the least-squares refinement was $\sum w(|F_o| - s|F_c|)^2$, where s was the inverse scale factor. The weight w of an observation was initially equated to $1/\sigma^2(F_o)$. Reflections whose intensities were below the observable threshold were given zero weights. The scattering factors for C, N, O, Cl^-, and Yb^{2+} were taken from Cromer and Waber.[7] Since the coordinated OH^- was represented by O^0 rather than O^-, a correct total electron count was maintained by using the scattering factor for Yb^{2+} in preference to that for Yb^{3+}. Both the real and imaginary parts of the correction for anomalous dispersion[8] were applied to the scattering factors of Cl^- and Yb^{2+}.

The refinement with isotropic atomic thermal parameters converged after three cycles. The values of the residuals[9] were $R_1 = R_2 = 0.061$. When anisotropic thermal parameters for the Yb and Cl atoms were introduced, the refinement converged with $R_1 = 0.052$ and $R_2 = 0.051$. After the third isotropic refinement cycle, it became evident that the standard deviations derived from the counting statistics alone did not reflect the true relative precisions of the structure amplitudes. At this stage and after all subsequent refinement cycles, new weights w for the observations were derived on the assumption that $w\Delta^2$ should vary systematically with neither $|F_o|$ nor $\sin\theta/\lambda$ ($\Delta = |F_o| - s|F_c|$). Range averages of $1/\Delta^2$ plotted against $\sin\theta/\lambda$ showed no systematic trends and the weights were adequately represented by $w = 1/[a + b|F_o| + c|F_o|^2]$. In the final refinement cycle the constants in this expression were $a = 6.38$, $b = -0.046$, $c = 0.000\,132$. The only interpretable features (≤ 1 e A^{-3}) in a final ($F_o - F_c$) synthesis appeared to be associated with vibrational anisotropy of some of the light atoms, but further refinement with additional anisotropic thermal parameters did not produce a significant drop in the residual R_1. The atomic parameters are listed in Table I.[10]

Computer Programs. The calculations were carried out using (i) programs for data reduction and Fourier synthesis written by J. F. Blount; (ii) the least-squares program ORFLS,[11] modified by J. A. Ibers to include a rigorous allowance for anomalous dispersion; and (iii) the stereoscopic plotting program ORTEP.[12]

Description of the Structure

The asymmetric unit consists of one Yb atom, a paphy molecule, two chloride ions, five water molecules and a hydroxyl ion. The chloride ions and two of the water molecules are not involved in the coordination of the metal atom. The remaining atoms form half of a centrosymmetric dimeric cation, $[Yb(paphy)(H_2O)_3(OH)]_2^{4+}$. The Yb atoms are eight coordinate. Each Yb atom is bonded to a tridentate paphy molecule and to five oxygen atoms. Two of these oxygens, O(1) and O(1′), are shared with the second Yb atom of the dimer. The two Yb atoms and the two bridging oxygen atoms form a planar four-membered ring. The distance between the metal atoms is 3.608 (1) Å. The paphy molecules are roughly perpendicular to the plane of the four-membered ring. A stereoscopic diagram of the environment of one Yb atom is shown in Figure 1. The bond lengths and selected bond angles

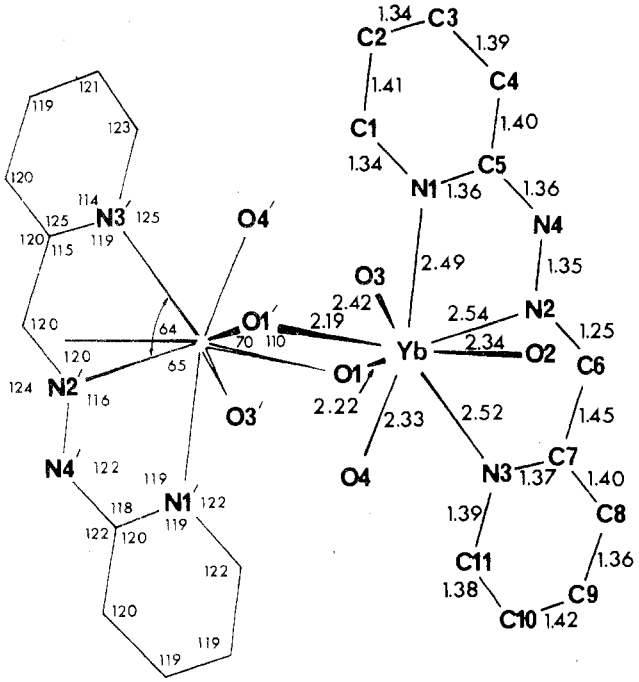

Figure 2. Geometry of the dimer, including the principal interatomic distances and bond angles. (Esd's are 0.01 Å for Yb–N and Yb–O; 0.02 Å for N–N, N–C, and C–C; 1° for bond angles at N atoms, 1.5° for bond angles at C atoms.)

Table II. Bond Angles (deg) at the Yb Atom in $[Yb(paphy)(H_2O)_3(OH)]_2^{4+}$

Atoms	Angle	Atoms	Angle
Yb-O(1)-Yb′	110.0 (3)	N(3)-Yb-O(1)	74.5 (3)
N(1)-Yb-N(2)	64.9 (3)	N(3)-Yb-O(1′)	133.1 (3)
N(1)-Yb-N(3)	128.6 (3)	N(3)-Yb-O(2)	76.9 (4)
N(1)-Yb-O(1)	92.4 (4)	N(3)-Yb-O(3)	140.2 (3)
N(1)-Yb-O(1′)	83.0 (4)	N(3)-Yb-O(4)	76.6 (3)
N(1)-Yb-O(2)	91.7 (4)	O(1)-Yb-O(1′)	70.0 (3)
N(1)-Yb-O(3)	75.7 (3)	O(1)-Yb-O(2)	146.3 (3)
N(1)-Yb-O(4)	153.5 (4)	O(1)-Yb-O(3)	142.3 (3)
N(2)-Yb-N(3)	63.8 (3)	O(1)-Yb-O(4)	103.9 (4)
N(2)-Yb-O(1)	78.6 (3)	O(1′)-Yb-O(2)	143.8 (4)
N(2)-Yb-O(1′)	133.7 (4)	O(1′)-Yb-O(3)	73.1 (3)
N(2)-Yb-O(2)	72.9 (3)	O(1′)-Yb-O(4)	83.2 (4)
N(2)-Yb-O(3)	124.6 (4)	O(2)-Yb-O(3)	70.8 (3)
N(2)-Yb-O(4)	138.3 (3)	O(2)-Yb-O(4)	86.3 (4)
		O(3)-Yb-O(4)	78.7 (3)

in the complex ion are summarized in Figure 2. A complete list of the bond angles at the Yb atom is given in Table II.

Coordination Geometry. The complex belongs to an important class of eight-coordinate lanthanide complexes in which the arrangement of the donor atoms is approximately dodecahedral (Figure 3).[13] The symmetry properties of the dodecahedron lead to distinctions between two types of vertices and four types of polyhedron edges.[13-15] In terms of the convention proposed by Hoard and Silverton,[14] the atoms N(2), N(3), O(1′), and O(3) occupy vertices of type A, while the atoms N(1), O(1), O(2), and O(4) lie at vertices of type B. The chemical differences between the eight donor atoms are such that the coordination geometry can scarcely be expected to conform precisely to that of a regular polyhedron. The limited "bites" of the tridentate paphy ligand impose additional constraints upon the geometry. The mean values of the metal–ligand bond lengths to type A and type B donor atoms are 2.42 (8) and 2.34 (6) Å, respectively, but there is a considerable scatter of values in each sample (Figure 2). The average lengths of the four types of dodecahedron edges,[14] followed by the maximum deviations from the individual values (Figure 3), are: $a = 2.71 \pm 0.04$, $b = 3.41 \pm 0.22$, $m = 2.75 \pm 0.26$, $g = 2.98 \pm 0.11$ Å.

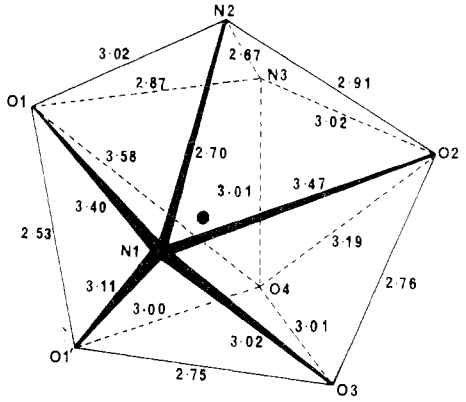

Figure 3. Dimensions of the coordination dodecahedron. Type A vertices: N(2), N(3), O(1′), O(3). Type B vertices: N(1), O(1), O(2), O(4). Type a edges: N(2)···N(3), O(1′)···O(3). Type b edges: N(1)···O(2), N(1)···O(1), O(4)···O(2), O(4)···O(1). Type m edges: N(2)···N(1), N(3)···O(4), O(3)···O(2), O(1′)···O(1). Type g edges: all others. For explanation of notation see ref 13.

The tridentate ligand occupies three adjacent and approximately coplanar corners of the coordination dodecahedron. The two smallest bond angles at the Yb atom are those subtended by the paphy donor atoms [N(1)–Yb–N(2) = 65°, N(2)–Yb–N(3) = 64°]. The mean Yb–N bond length is 2.52 Å. The differences between the lengths of the Yb–N(pyridine) bonds (2.49 (1), 2.52 (1) Å) and the Yb–N(imine) bond (2.54(1) Å) are not significant. In the complexes Co(paphy)Cl_2 (square pyramidal)[16] and Mo(paphy)$(CO)_4$ (octahedral),[17] the metal–N(pyridine) and metal–N(imine) bond lengths are also approximately equal.

The Yb–O bond lengths, on the other hand, fall into two categories. The bonds Yb–O(1) and Yb–O(1′) in the four-membered ring at the center of the dimer are more than 0.1 Å shorter than the remaining Yb–O bonds (Figure 2). Since the bridging oxygen atoms each form two strong metal–oxygen bonds, their basicity should be lowered in comparison with singly bonded oxygens. Accordingly, the oxygen atoms O(1) and O(1′) are assigned to hydroxyl groups and the oxygen atoms O(2), O(3), and O(4) to water molecules. The hydrolysis of hydrated cations to form hydroxyl-bridged dimers is a well-known phenomenon.

Geometry of the paphy Molecule. Within the limits of precision of the structure analysis, the pyridine rings have normal dimensions (Figure 2 and Table II) and do not deviate significantly from planarity. The bond lengths in the carboxaldehyde hydrazone chain, C(7)–C(6)–N(2)–N(4)–C(5), indicate that all four bonds have considerable double-bond character. The bond lengths and angle involving N(4) are consistent with a state of hybridization close to sp^2.

The Yb atom lies at 0.06 and 0.32 Å from the planes of the pyridine rings which contain N(1) and N(3), respectively. The resulting nonplanarity of the Yb–paphy portion of the complex no doubt relieves strains in the two adjacent five-membered chelate rings. The most pronounced fold of the paphy molecule is about the line joining the Yb and C(6) atoms (Figure 4).[18]

Hydrogen Bonds and Nonbonded Contacts. The hydrogen bonds are listed in Table III. The description of the bonds in terms of proton donors and acceptors is unequivocal. Each of the three coordinated water molecules O(2), O(3), and O(4) forms two hydrogen bonds in which it is the proton donor. Each of the two lattice water molecules O(5) and O(6) accepts one hydrogen bond from a coordinated water molecule, and acts as a proton donor in two O–H···Cl hydrogen bonds with chloride ions. The bridging hydroxyl groups do not form hydrogen bonds. The chloride ions Cl(1) and Cl(2) are each hydrogen bonded to four water molecules. The bond angles

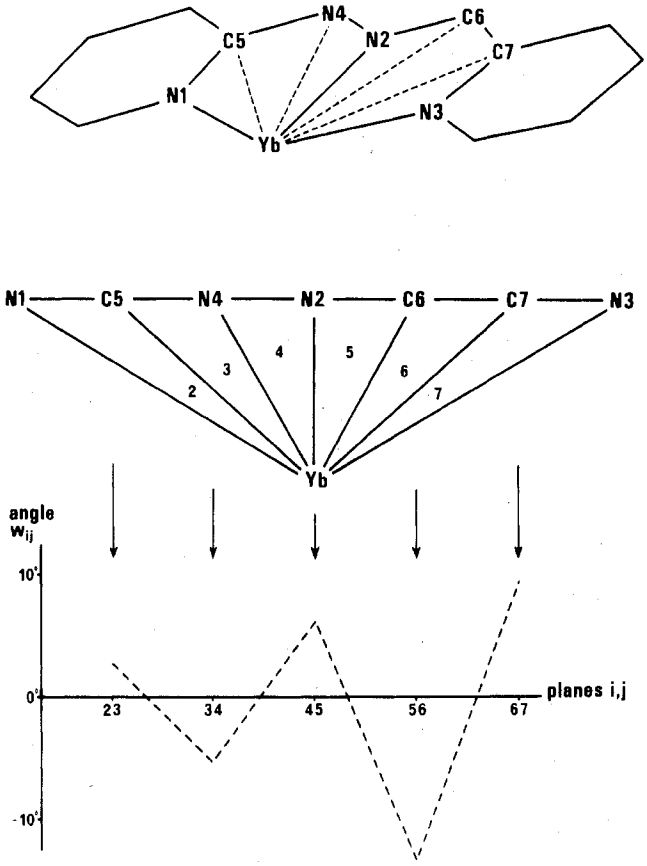

Figure 4. Conformations of the Yb-paphy chelate rings. The chelate rings are divided into triangles having the Yb atom as a common vertex. The planes fitted to these triangles are numbered as shown. The dihedral angle ω_{ij} between two adjacent planes i and j is positive if the plane i is brought into coincidence with the plane j by a clockwise rotation about their line of intersection. The sense of rotation is defined with respect to an observer looking from the metal atom to the periphery of the complex. The values of the angles $\omega_{12}, \omega_{23}, \cdots$ are 2.9, −5.3, 6.0, −13.3, and 9.7°.

Table III. Hydrogen Bonds

Symmetry Transformations with Respect to the Coordinates Listed in Table I

Superscript	Atom at	Superscript	Atom at
	x, y, z	iv	$^1/_2 - x, -y, -^1/_2 + z$
i	$-x, -y, -z$	v	$x, ^1/_2 - y, -^1/_2 + z$
ii	$^1/_2 - x, -^1/_2 + y, z$	vi	$-x, -^1/_2 + y, ^1/_2 - z$
iii	$^1/_2 - x, ^1/_2 + y, z$		

Hydrogen Bond Lengths, Å

Atoms X-H···Y	d(X···Y)	Atoms X-H···Y	d(X···Y)
O(2)-H···O(5)	2.69	O(5)-H···Cl(1)	3.19
O(2)-H···Cl(2^{ii})	3.13	O(5)-H···Cl(2)	3.20
O(3)-H···Cl(1^{iv})	3.15	O(6)-H···Cl(1)	3.18
O(3)-H···Cl(2^{ii})	3.21	O(6)-H···Cl(1^{iii})	3.24
O(4)-H···O(6^{v})	2.66	N(4)-H···O(5^{vi})	3.05
O(4)-H···Cl(2)	3.19		

at the hydrogen-bonded atoms (including the angles between covalent bonds and hydrogen bonds) are in the ranges: O(2), 111–130°; O(3), 112–130°; O(4), 113–124°; O(5), 89–139°; O(6), 103–134°; N(4), 113–122°; Cl(1), 72–149°; Cl(2), 52–151°.

The shortest nonbonded intermolecular contact is C(9)···N(4^{ix}) (3.24 Å). There are two short nonbonded intracomplex contacts between the paphy molecule and coordinated water molecules, C(1)···O(3) and C(11)···O(4) (3.09, 3.09 Å).

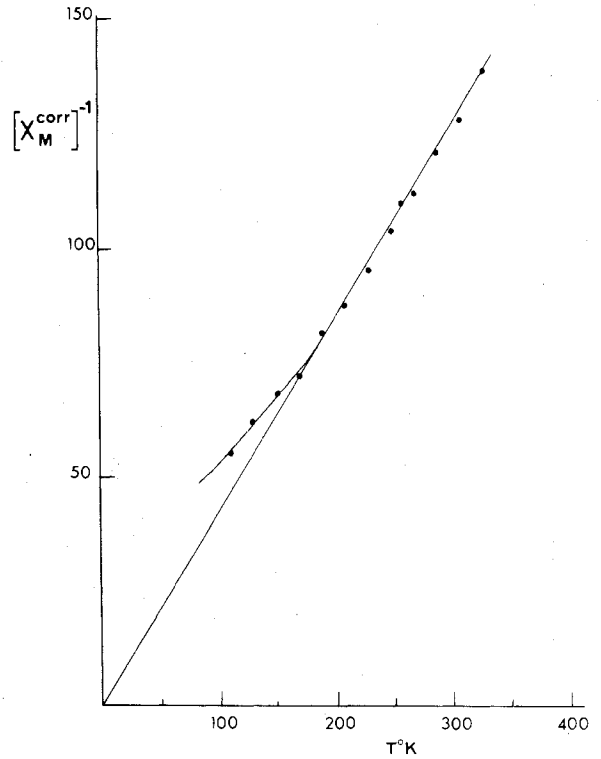

Figure 5. Temperature dependence of the inverse magnetic susceptibility.

Discussion of Physical Properties

Infrared Spectra.[10] The spectrum recorded by us for the free ligand is in substantial agreement with that reported by Bell and Rose,[19] and we have followed these authors' assignment of the frequencies. The vibrational frequencies in the spectrum of the complex can then be made on the basis of a qualitative comparison with the spectrum of the ligand. Among the five vibrational modes of pyridine in the region between 1650 and 950 cm^{-1}, the breathing mode near 1000 cm^{-1} is the one which is most sensitive to metal binding at the pyridine nitrogen atom.[1] The two components of this band in the spectrum of paphy occur at 995 sh and 991 m cm^{-1}. Both components undergo shifts to 1012 m and 1001 m cm^{-1} when the ligand becomes bonded to Yb. These shifts are consistent with the participation of the two pyridine rings of paphy in the tridentate chelation.

In the far-infrared region between 400 and 30 cm^{-1}, the fact that the crystal structure of the complex is known enables us to make a tentative assignment of the Yb–N stretching frequency. Unequivocal assignments of lanthanide–N frequencies have hitherto been difficult because lanthanide–halide stretching modes are believed to occur in the same region of the spectrum (350–250 cm^{-1}) and to have greater intensities.[20] In the present complex the chloride ions are not bonded to the Yb atom. The bands which are characteristic of Yb–O bonds are known to occur between 400 and 500 cm^{-1}.[21] Accordingly, a strong band at 299 cm^{-1} with satellites at 305 m, 290 sh, and 275 sh cm^{-1} can be assigned to Yb–N(stretch).

Magnetic Susceptibility. The temperature dependence of the reciprocal of the molar magnetic susceptibility is shown in Figure 5. The value of μ_{eff} is 4.43 BM, in agreement with the theoretical value of 4.54 BM for Yb(III).[22] The magnetic susceptibility therefore requires the presence of one negative charge in addition to the two Cl^- ions per Yb atom. The identification of the bridging OH^- ions as the sources of the additional negative charge in the complex has already been discussed. There is no evidence that the internuclear distance of 3.609 Å between the two Yb atoms of the dimer leads to

Table IV. Uv-Visible Absorption Bands ($cm^{-1} \times 10^{-3}$) of paphy, $[Yb(paphy)(H_2O)_3(OH)]_2Cl_4 \cdot 4H_2O$ (Complex A), and Dehydration Product (complex B), Recorded as Nujol Mulls

	Paphy	Complex A	Complex B
Band I	42.3	38.8	35.8
		32.1	31.8
Band II	29.9	27.2 (sh)	26.4 (sh)
		24.8 (sh)	21.8 (sh)

any magnetic interaction at temperatures above 220 K. Below this temperature there is a small deviation from Curie–Weiss behavior. The magnetic properties of the complex between 4 and 90 K are being studied further. In a chloro-bridged dimeric complex with a Yb–Yb separation of 3.98 Å, Raymond found no magnetic interaction between the Yb(III) atoms at temperatures down to 4 K.[23,24]

Ultraviolet–Visible Spectra. The solid-state uv–visible spectra of the free ligand, the complex, and the final dehydration product obtained after prolonged heating and the loss of four H_2O per Yb are summarized in Table IV. The spectrum of the free ligand has two strong bands. These bands split and undergo large bathochromic shifts when the ligand becomes coordinated to Yb(III). The bands move to even longer wavelengths in the dehydration product. The stepwise dehydration of the complex (see Experimental Section) is consistent with the initial loss of two molecules of lattice H_2O per Yb atom, followed by the loss of two coordinated H_2O molecules per Yb atom. A reduction of the coordination number of Yb from 8 to 6 would account for the large bathochromic shift on dehydration.

Acknowledgment. Financial support from the Australian Research Grants Committee (Grant 65/15552) and from the U.S. Public Health Service (Grant GM-10867) is gratefully acknowledged.

Registry No. A, 59738-47-5; B, 59738-48-6.

Supplementary Material Available: Listings of (i) the infrared spectroscopic data for paphy and $[Yb(paphy)(H_2O)_3(OH)]_2Cl_4 \cdot 4H_2O$ and (ii) the x-ray structure factor amplitudes for $[Yb(paphy)(H_2O)_3(OH)]Cl_2 \cdot 2H_2O$ in $[Yb(paphy)(H_2O)_3(OH)]_2Cl_4 \cdot 4H_2O$ (22 pages). Ordering information is given on any current masthead page.

References and Notes

(1) E. Baraniak and J. M. James, unpublished work.
(2) B. N. Figgis and J. Lewis, "Modern Coordination Chemistry", J. Lewis and R. G. Wilkins, Ed., Interscience, New York, N.Y., 1960, p 403.
(3) H. C. Freeman, J. M. Guss, C. E. Nockolds, R. Page, and A. Webster, *Acta Crystallogr., Sect. A*, **26**, 149 (1970).
(4) W. C. Hamilton, *Acta Crystallogr.*, **8**, 185 (1955).
(5) P. Coppens, L. Leiserowitz, and D. Rabinovich, *Acta Crystallogr.*, **18**, 1035 (1965).
(6) A. D. Rae, *Acta Crystallogr.*, **19**, 683 (1965); A. D. Rae and A. B. Blake, *ibid.*, **20**, 586 (1966).
(7) D. T. Cromer and J. T. Waber, *Acta Crystallogr.*, **18**, 104 (1965).
(8) D. T. Cromer, *Acta Crystallogr.*, **18**, 17 (1965).
(9) $R_1 = \sum||F_o| - s|F_c||/\sum|F_o|$; $R_2 = [\sum w||F_o| - s|F_c||^2/\sum w|F_o|^2]^{1/2}$.
(10) See paragraph regarding supplementary material.
(11) W. R. Busing, K. O. Martin, and H. A. Levy, Report ORNL-TM-305, Oak Ridge National Laboratory, Oak Ridge, Tenn., 1962.
(12) C. K. Johnson, Document ORNL-3794, Oak Ridge National Laboratory, Oak Ridge, Tenn., 1965.
(13) S. P. Sinha, "Structure and Bonding", Vol. 25, J. D. Dunitz et al., Ed., Springer, Berlin, 1975, p 69.
(14) J. L. Hoard and J. V. Silverton, *Inorg. Chem.*, **2**, 235 (1963).
(15) S. J. Lippard, *Prog. Inorg. Chem.*, **8**, 109 (1967).
(16) M. Gerloch, *J. Chem. Soc. A*, 1317 (1966).
(17) R. St. L. Bruce, M. K. Cooper, H. C. Freeman, and B. G. McGrath, *Inorg. Chem.*, **13**, 1032 (1974).
(18) Details and advantages of the method used to represent chelate ring conformations in Figure 4 are discussed by H. C. Freeman, M. J. Healy, and M. L. Scudder, *J. Biol. Chem.*, in press.
(19) C. F. Bell and D. R. Rose, *Inorg. Chem.*, **7**, 325 (1968).
(20) L. J. Basile, D. L. Gronert, and J. R. Ferraro, *Spectrochim. Acta, Part A*, **24**, 707 (1968).
(21) J. Ferraro, *Anal. Chem.*, **40**, 24A (1968).
(22) J. H. Van Vleck and A. Frank, *Phys. Rev.*, **34**, 1494 (1929).
(23) E. C. Baker, L. D. Brown, and K. N. Raymond, *Inorg. Chem.*, **14**, 1376 (1975).
(24) K. N. Raymond, personal communication.

Contribution from the Department of Chemistry, University of Iowa, Iowa City, Iowa 52242

Crystal and Molecular Structure of Bis[bis(diphenylethylphosphine)silver(I)] Bis(1,2-dicyano-1,2-ethylenedithiolato)nickelate(II), $[Ag(P(C_6H_5)_2(C_2H_5))_2]_2Ni(S_2C_2(CN)_2)_2$. Steric Effects on the P–Ag–P Angle

F. J. HOLLANDER, Y. L. IP, and D. COUCOUVANIS*

Received February 19, 1976 AIC60134V

Bis[bis(diphenylethylphosphine)silver(I)] bis(1,2-dicyano-1,2-ethylenedithiolato)nickelate(II), $[Ag(P(C_6H_5)_2(C_2H_5))_2]_2Ni(S_2C_2(CN)_2)_2$, crystallizes in the orthorhombic space group *Pbca* with four molecules per unit cell. The cell dimensions are $a = 18.427$ (9) Å, $b = 26.894$ (10) Å, and $c = 13.149$ (9) Å. Intensity data were collected with a four-circle computer-controlled diffractometer using the θ–2θ scan technique. All 40 nonhydrogen atoms were refined anisotropically and the 30 hydrogen atoms were included as fixed atoms. Refinement by full-matrix least squares using 2113 reflections gave an R value of 0.023 for 358 parameters. The geometry of the NiS_4 group is square planar. The interaction of $Ag(PPh_3)_2^+$ occurs at the NiS_4 group and the silver atoms are located above and below the NiS_4 plane in a chair configuration. Average values of selected bond distances and angles in the $(AgP_2)_2NiS_4$ core are as follows: Ag–Ni = 2.986 Å, Ag–S = 2.854 Å, Ni–S = 2.177 Å, Ag–P = 2.449 Å, Ni–Ag–S = 43.70°, S–Ni–S(interligand) = 87.55°, S–Ni–S(intraligand) = 92.45°, P–Ag–P = 128.00°. The ^{31}P NMR spectra of the $[(P(C_6H_5)_n(C_2H_5)_{3-n})_2Ag]_2Ni(mnt)_2$ complexes ($n = 0, 1, 2, 3$) were obtained and the ^{107}Ag–^{31}P coupling constants were 394, 413, 426, and 426 Hz for $n = 3$, 2, 1, and 0, respectively. These data when correlated to P–Ag–P angle values indicate the importance of steric effects in determining the s character of the Ag–P bond.

Introduction

In a recent study of the solution structure of silver(I)–phosphine complexes, Muetterties and Alegranti[1] presented some interesting conclusions about the structural and kinetic features of these compounds. A notable characteristic in the ^{31}P nuclear magnetic resonance spectra of the $((tol)_3P)_2AgL$ complexes was the variation in magnitude of the Ag–^{31}P coupling constants. Thus values from 380 to 470 Hz were observed in compounds for which conductivity studies did not indicate an appreciable extent of dissociation (eq 1).

$$(P(tol)_3)_2AgL \rightleftarrows (P(tol)_3)_2Ag^+ + L^- \quad (1)$$

The values of the Ag–P coupling constant, to a first approximation, can be correlated with the percent s character